

Presented at the SPIE 33rd Annual International Technical Symposium on Optical and Optoelectronic Applied Science and Engineering, "Optical Materials Technology for Energy Efficiency and Solar Energy Conversion VIII," San Diego, CA, August 6–11, 1989, and to be published in the Proceedings

Chromatic Dispersion Compensation in a Fresnel Lens by Means of a Diffraction Grating

K.C. Johnson

August 1989

Presented at the SPIE Optical Materials Technology for Energy Efficiency and Solar Energy Conversion VIII,
August 1989, San Diego, CA.

Chromatic dispersion compensation in a Fresnel lens by means of a diffraction grating

Kenneth C. Johnson

Lawrence Berkeley Laboratory, Applied Science Division
1 Cyclotron Road, Berkeley, CA 94720

August 1989

This work was supported by the Assistant Secretary for Conservation and Renewable Energy, Office of Solar Heat Technologies, Solar Buildings Division of the U.S. Department of Energy under Contract No. DE-AC03-76SF00098.

Chromatic dispersion compensation in a Fresnel lens by means of a diffraction grating

Kenneth C. Johnson

Lawrence Berkeley Laboratory, Applied Science Division
1 Cyclotron Road, Berkeley, CA 94720

ABSTRACT

A Fresnel lens's imaging performance can be seriously impaired by chromatic dispersion which typically doubles the diameter of the focused sun image in a solar concentrator. This problem can be alleviated by means of a molded diffraction grating whose diffraction-induced dispersion offsets and substantially cancels the lens's intrinsic refractive index dispersion. The grating lines would comprise a second tier of small-scale, Fresnel-type facets superimposed on the lens facets, with a typical grating facet height of about 40 microinches and a facet width ranging from about 1 milliinch at the edge of the lens to around 5 or 10 milliinches near the center. In its primary intended application the grating would function in a core daylighting system to improve the optical performance of a collector which focuses direct sunlight into fiber optic couplers. For this application chromatic dispersion would be reduced by an order of magnitude with only a 2% loss in optical efficiency.

1. INTRODUCTION

An acrylic lens generally exhibits a significant degree of chromatic dispersion, with blue light being more strongly diffracted than red. The chromatic dispersive spread in a ray is roughly proportional to the angle by which the ray is deviated via refraction, and is typically around 0.5° (for a white-light spectrum) near the edge of a Fresnel lens of focal ratio 1.

Another mechanism that also exhibits chromatic dispersion is a diffraction grating, which tends to diffract red light more strongly than blue. The dispersive spread in a diffracted ray is roughly proportional to the grating's spatial frequency and is comparable to an acrylic lens's refractive dispersion when the grating has a very low spatial frequency in the range of 1000 lines per inch or less.

By forming a diffraction grating directly on the surface of a lens and optimally balancing the element's refractive and diffractive optical power, its chromatic dispersion can be substantially reduced and can be precisely eliminated at two specific design wavelengths. This method has been used by Stone and George¹ to achromatize conventional (non-Fresnel) lenses using volume holographic gratings; however holographic gratings have practical limitations which make them unsuitable for solar applications. Dispersion compensation in a Fresnel lens can be more practically achieved by means of a blazed transmission grating formed as a molded relief pattern on the lens surface.*

Fig. 1 illustrates the facet structure of a dispersion-compensated Fresnel lens. (The figure shows a sectional view of an axially-symmetric element.) The lens profile has a two-tiered facet structure comprising large-scale (e.g. 0.05-inch) annular lens facets on which are superimposed small-scale grating facets. The grating facets themselves comprise a Fresnel-type pattern of annular facets, but with microscopic facet dimensions and extremely shallow facet profiles. The grating's

* patent pending

line density varies approximately linearly with lens radius, with a maximum density of about 1000 lines per inch for an acrylic lens of focal ratio 1. (The grating need not extend over the center of the lens since dispersion is generally negligible near the lens axis.) The grating's facet height is around 40 microinches over the full lens aperture.

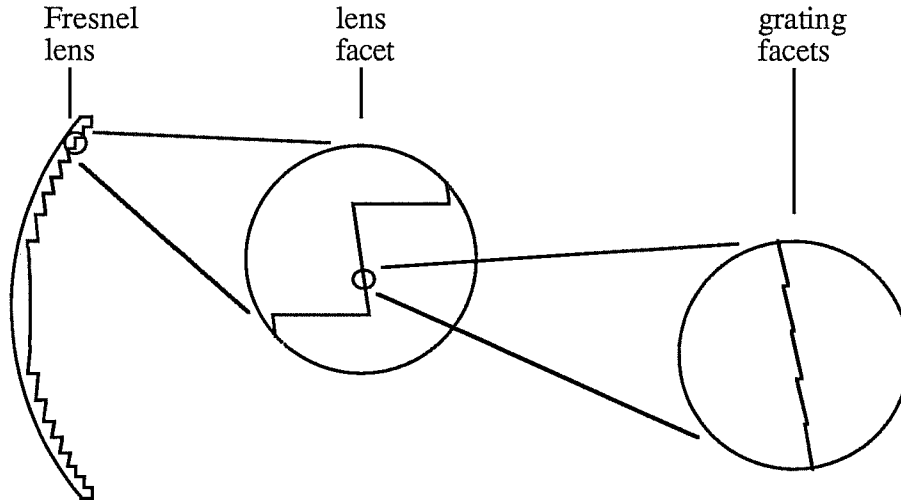


Fig. 1. Cross-section of a dispersion-compensated Fresnel lens

Since the grating structure may be formed directly in the lens molding tool, no extra manufacturing steps are required to fabricate the grating. The grating's facet dimensions are very small in comparison to conventional Fresnel lens facets, but its spatial frequency is an order of magnitude lower than that of typical spectroscopic gratings and its profile is extremely shallow, so no modification of conventional lens molding processes would be required to form the grating. (Due to uncommonly stringent tolerances in the grating facet dimensions, however, state-of-the-art diamond turning facilities would be required for tooling the lens mold.)

2. THEORY

The design and optical performance of a blazed transmission grating are determined by two relations: the standard grating equation which determines the dispersion characteristics of gratings in general, and a diffraction efficiency equation which applies specifically to blazed gratings. The following parameters enter into these relations:

Λ	grating period
α	grating facet angle
λ	wavelength (in air)
θ	incidence angle (relative to grating substrate)
θ'	exit angle (relative to grating substrate)
n	refractive index in incidence medium
n'	refractive index in exit medium

(n and n' may be functions of λ .) Fig. 2 shows a microscopic section of a blazed grating illustrating these parameters. The figure represents a small, localized region of the grating over which the grating structure is essentially uniform with approximately straight, parallel facets and the incident beam is approximately collimated. The grating surface separates two optical media, the incidence and exit media, whose refractive indexes are n and n' , respectively. An incident beam of

wavelength λ (in air) impinges on the grating at an incidence angle θ relative to the grating "substrate" (an imaginary base plane tangent to the grating) and is scattered into a number of diffracted orders, one of which is illustrated as exiting the grating at an angle θ' relative to the substrate.

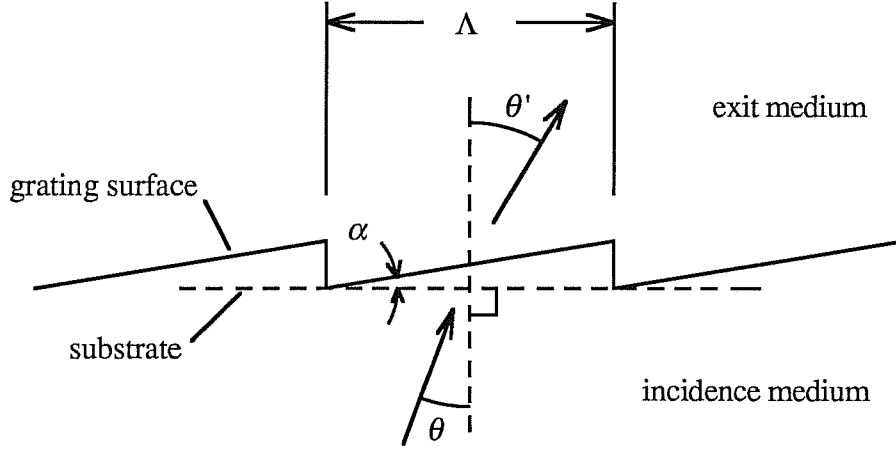


Fig. 2. Diffraction geometry of a blazed transmission grating

2.1 Dispersion

The grating equation for the m -th diffracted order is

$$n' \sin \theta' = n \sin \theta + m \lambda / \Lambda. \quad (1)$$

A dispersion-compensating grating would normally use only the first or minus first diffracted order, so m would be ± 1 in equation (1). (Λ is conventionally defined as a signed quantity with its sign chosen so that the active order is a plus first order.) Note that equation (1) reduces to Snell's Law when Λ approaches infinity. For a dispersion-compensating grating the term λ / Λ in (1) would be very small (around 0.02 or less) but its wavelength dependence would nevertheless have a significant influence on the element's chromatic dispersion. The grating structure is designed so that the wavelength dependence of n and/or n' is offset and substantially canceled by the λ / Λ term.

The two degrees of freedom afforded by the choice of the grating period and substrate orientation make it possible to eliminate chromatic dispersion between two specific design wavelengths. For two particular design wavelengths, λ_1 and λ_2 , the first order grating equation ($m = 1$) takes the form,

$$n'_1 \sin \theta'_1 = n_1 \sin \theta_1 + \lambda_1 / \Lambda \quad (2)$$

$$n'_2 \sin \theta'_2 = n_2 \sin \theta_2 + \lambda_2 / \Lambda \quad (3)$$

where the subscripted parameters are associated with the corresponding wavelengths. The two incidence angles θ_1 and θ_2 may diverge slightly by a specified angle $\Delta\theta$ due to the effect of

chromatic dispersion at any optical surfaces preceding the grating (such as the first surface of a Fresnel lens, if the grating is formed on its second surface):

$$\Delta\theta = \theta_2 - \theta_1. \quad (4)$$

The incidence and exit angles are not initially specified, but the ray deflection angles φ_1 and φ_2 at wavelengths λ_1 and λ_2 are predetermined:

$$\varphi_1 = \theta'_1 - \theta_1 \quad (5)$$

$$\varphi_2 = \theta'_2 - \theta_2 \quad (6)$$

φ_1 and φ_2 may be chosen to induce a slight predetermined divergence angle $\Delta\theta'$ between the exit angles θ'_1 and θ'_2 to compensate for chromatic dispersion at any optical surfaces following the grating (such as the second surface of a Fresnel lens, if the grating is formed on its first surface):

$$\Delta\theta' = \theta'_2 - \theta'_1 = \Delta\theta + \varphi_2 - \varphi_1 \quad (7)$$

The grating parameters are calculated by solving the five relations (2) - (6) for the five unknowns θ_1 , θ_2 , θ'_1 , θ'_2 and Λ . Using (4) - (6) to eliminate θ_2 , θ'_1 and θ'_2 in (2) and (3) and then eliminating Λ between (2) and (3) and isolating θ_1 , we obtain

$$\tan \theta_1 = \frac{\lambda_2(n'_1 \sin(\varphi_1)) - \lambda_1(n'_2 \sin(\Delta\theta + \varphi_2) - n_2 \sin(\Delta\theta))}{\lambda_2(n_1 - n'_1 \cos(\varphi_1)) + \lambda_1(n'_2 \cos(\Delta\theta + \varphi_2) - n_2 \cos(\Delta\theta))} \quad (8)$$

Having determined θ_1 , θ'_1 is determined by (5), Λ is determined by (2), θ_2 is determined by (4), and θ'_2 is determined by (6).

2.2 Efficiency

A blazed transmission grating's diffraction efficiency η in the m -th diffracted order is approximately

$$\eta = \text{sinc}^2\left(\pi \frac{\Lambda}{\lambda} n' (\sin \theta'_{\text{Snell}} - \sin \theta')\right) \quad (9)$$

(neglecting surface reflection losses) where θ' is the m -th order's exit angle as defined by equation (1) and θ'_{Snell} is the exit angle defined by Snell's Law at the grating facet surface:

$$n' \sin(\theta'_{\text{Snell}} + \alpha) = n \sin(\theta + \alpha) \quad (10)$$

Although Snell's Law does not apply to diffraction gratings, it is consistent with the grating equation since equation (9) predicts that when the grating period is very large ($\Lambda \gg \lambda$) the only diffracted orders of significant intensity are those with exit angles θ' very close to θ'_{Snell} .

Eliminating θ' between (1) and (9), we obtain the following equivalent expression for η :

$$\eta = \text{sinc}^2\left(\pi\left(\frac{\lambda_B}{\lambda} - m\right)\right) \quad (11)$$

where the "blaze wavelength" λ_B is obtained from the grating equation (1) with the substitutions $\lambda = \lambda_B$, $\theta' = \theta'_{Snell}$ and $m = 1$:

$$\lambda_B = \Lambda(n' \sin \theta'_{Snell} - n \sin \theta) \quad (12)$$

(The sign of Λ is conventionally chosen so that λ_B is positive.) For first-order diffraction ($m = 1$), efficiency is maximized and equal to 1 when $\lambda = \lambda_B$ (i.e. when $\theta' = \theta'_{Snell}$). The blaze wavelength λ_B is determined by the grating's facet angle α , and if λ_B is specified α can be calculated by solving equation (12) for θ'_{Snell} and substituting this value into relation (10) to solve for α . The following equivalent form of relation (10) is useful for calculating α :

$$\tan \alpha = \frac{\lambda_B}{\Lambda(n \cos \theta - n' \cos \theta'_{Snell})} \quad (13)$$

3. APPLICATIONS

For each of the applications considered below comparative optical performance data will be presented for two optical configurations (Fig. 3): a conventional configuration in which a ray is deflected via refraction at two surfaces of a prism, and a similar dispersion-compensated configuration in which the prism's second (bottom) refracting surface is replaced by a dispersion-compensating diffraction grating. For each configuration the ray's deflection angle φ_{top} at the top prism surface and its deflection angle φ_{bottom} at the bottom surface can be determined by application of Snell's Law and the grating equation. The total deflection angle φ_{total} is

$$\varphi_{total} = \varphi_{top} + \varphi_{bottom}. \quad (14)$$

The deflection angles are functions of wavelength, so we also define the spectrally-averaged deflection angles,

$$\overline{\varphi_{top}} = \left(\int W_\lambda \cdot \varphi_{top} d\lambda \right) / \left(\int W_\lambda d\lambda \right) \quad (15)$$

$$\overline{\varphi_{bottom}} = (\int W_{\lambda} \cdot \varphi_{bottom} d\lambda) / (\int W_{\lambda} d\lambda) \quad (16)$$

$$\overline{\varphi_{total}} = (\int W_{\lambda} \cdot \varphi_{total} d\lambda) / (\int W_{\lambda} d\lambda) = \overline{\varphi_{top}} + \overline{\varphi_{bottom}} \quad (17)$$

where W_{λ} is a spectral weighting function which is a measure of the efficiency with which radiation at wavelength λ is utilized. The optical geometries of both configurations are chosen so that $\overline{\varphi_{top}} = \overline{\varphi_{bottom}} = 15^{\circ}$, for a total deflection angle $\overline{\varphi_{total}} = 30^{\circ}$. (This represents a typical optical configuration for a ray near a curved Fresnel lens's edge where dispersion is worst.)

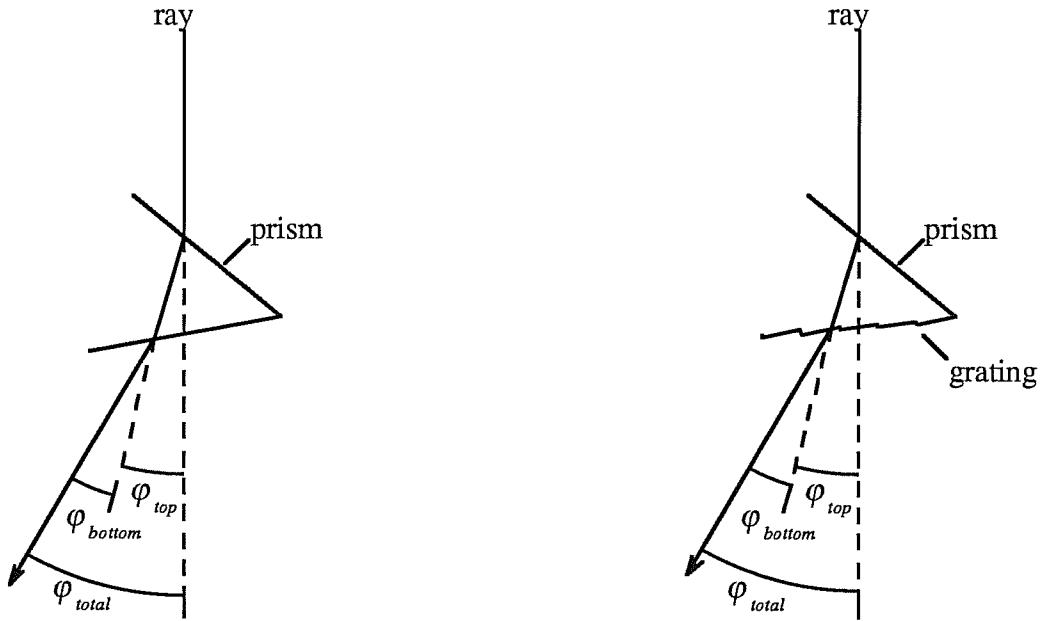


Fig. 3. Conventional configuration

Dispersion-compensated configuration

Each configuration's chromatic dispersion is characterized by calculating the mean-square deviation of φ_{total} ,

$$\overline{(\varphi_{total} - \overline{\varphi_{total}})^2} = (\int W_{\lambda} \cdot (\varphi_{total} - \overline{\varphi_{total}})^2 d\lambda) / (\int W_{\lambda} d\lambda) \quad (18)$$

and quantifying the dispersion in terms of $\Delta\varphi_{total}$, the root-mean-square deviation of φ_{total} :

$$\Delta\varphi_{total} = \sqrt{\overline{(\varphi_{total} - \overline{\varphi_{total}})^2}}. \quad (19)$$

The grating configuration's optical performance is also quantified in terms of its spectrally-averaged diffraction efficiency $\bar{\eta}$, defined as

$$\bar{\eta} = (\int W_{\lambda} \cdot \eta \, d\lambda) / (\int W_{\lambda} \, d\lambda) \quad (20)$$

where η is the first-order diffraction efficiency at wavelength λ (equation (9)). This efficiency measure does not include effect of surface reflections; however the grating's reflectance loss is essentially equivalent to that of a conventional refracting surface so $\bar{\eta}$ represents a meaningful efficiency measure if we take the conventional configuration's efficiency to be 1.

3.1 Core daylighting

The illuminance level of direct sunlight is around one hundred times greater than typical indoor lighting levels; hence there is considerable potential for energy savings through direct use of sunlight for daylighting. A "core daylighting system" uses tracking solar concentrators and light guides to channel direct sunlight to deep interior building regions where daylight would not normally penetrate. In combination with automatically dimmable artificial illumination, a core daylighting system can provide quality indoor lighting and could potentially displace all or most of a building's electric lighting load during periods of sunshine availability.

Two core daylighting systems are currently in operation including one commercial system^{2,3}. These systems are not currently cost-effective on the basis of their energy savings; however a design concept for a potentially cost-effective system has recently been developed by Lawrence Berkeley Laboratory's Windows and Daylighting Group. This system would use Fresnel lens concentrators to channel spectrally-filtered sunlight into acrylic optical fiber couplers at very high geometric concentration. The system's cost-effectiveness is significantly influenced by the required aggregate optical fiber aperture area, which is very sensitive to the lens's chromatic dispersion; hence dispersion correction can significantly enhance the system's cost-effectiveness.

In characterizing a daylighting system's optical performance, the appropriate spectral weighting factor W_{λ} is the spectral illuminance of direct sunlight, which can be calculated by multiplying the solar spectral irradiance* by the photopic spectral luminous efficacy⁵. For an

* For all three applications analyzed in Sect. 3 the solar spectral irradiance was calculated using the model developed by Bird and Riordan⁴, with the following parameters:

Latitude: 37°, Longitude: 100°
 Day number (1...365): 172
 Zenith angle: 13.56°
 Pressure: 1013 mb
 Water vapor: 0.5 cm
 Turbidity at 0.5 μ m: 0.1

For these parameters the direct normal solar irradiance is 960 W/m² and the illuminance is 102431 lm/m². (There is a slight but insignificant improvement in the grating's optical performance at lower irradiance levels.)

acrylic optical medium* the following performance data were calculated for the two configurations of Fig. 3**: For the conventional configuration $\Delta\varphi_{total} = 0.145^\circ$, and with dispersion compensation $\Delta\varphi_{total} = 0.026^\circ$. The grating's efficiency is $\bar{\eta} = 0.981$; hence dispersion is reduced by a factor of 6 at a cost of 2% efficiency loss. Fig. 4 illustrates the wavelength dependence of φ_{total} for both configurations and Fig. 5 illustrates the grating's efficiency characteristic in comparison the solar spectral illuminance.

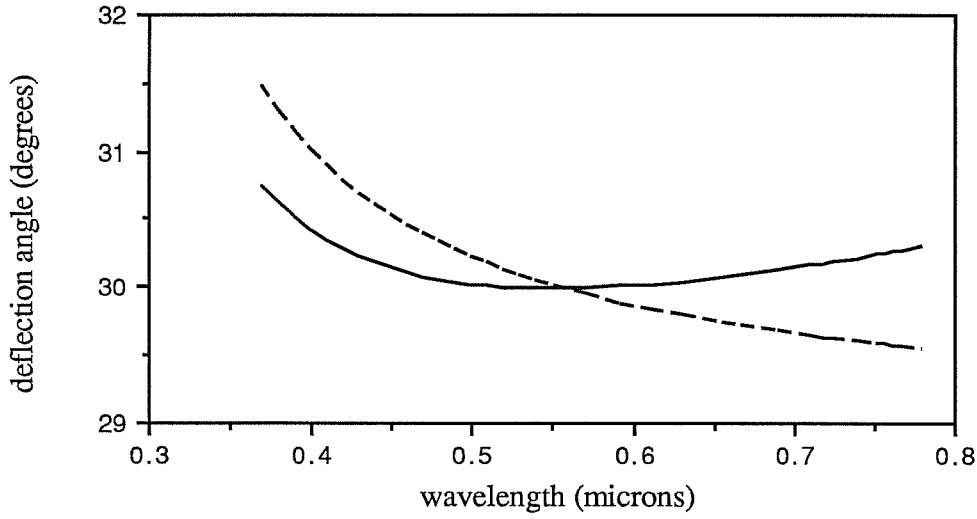


Fig. 4. Daylighting application: dispersion characteristic for the conventional configuration (dashed line; $\Delta\varphi_{total} = 0.145^\circ$) vs. dispersion-compensated configuration (solid line; $\Delta\varphi_{total} = 0.026^\circ$)

* The refractive index of acrylic was calculated using the following empirical formula:

$$n = 0.005313/(\lambda - 0.2307\mu\text{m}) + 1.4768$$

(The coefficients in this expression were chosen to match the data in Ref. 6.)

** For both configurations the incidence angle at the top surface is 41.14° . The prism facet angle is 52.28° for the conventional configuration and 49.89° for the dispersion-compensated configuration. The grating's period is $22.73\mu\text{m}$ and its facet angle is 2.37° . (These parameters were chosen to minimize $\Delta\varphi_{total}$ and maximize $\bar{\eta}$.)

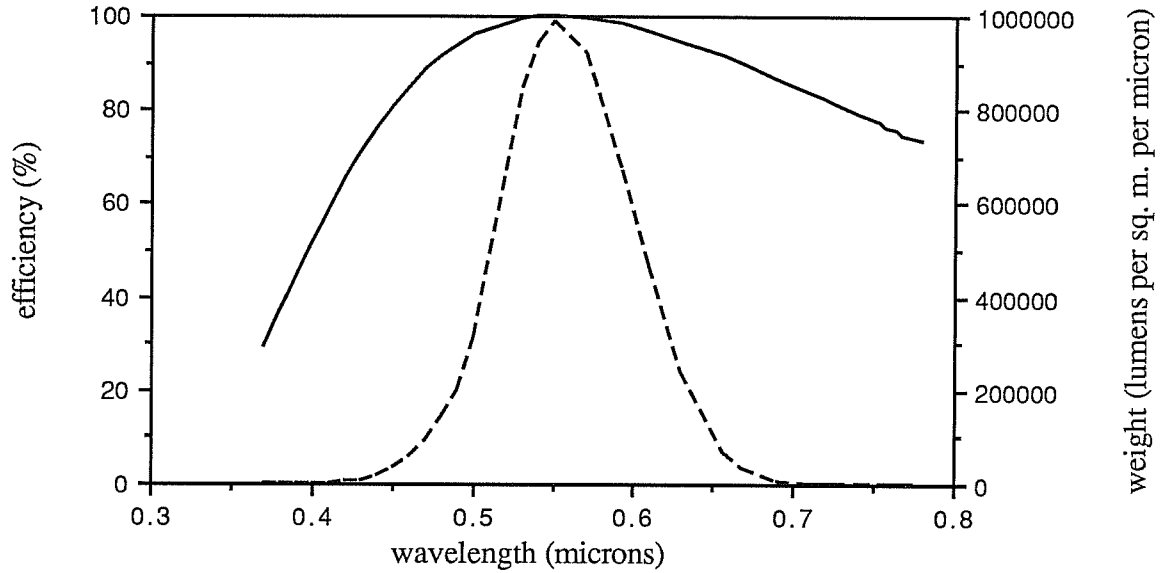


Fig. 5. Grating efficiency (solid line) vs. photopic weighting function (dashed line); $\bar{\eta} = 0.981$

3.2 Concentrator photovoltaics

Dispersion-compensating gratings could significantly increase the optical concentration in gallium-arsenide (GaAs) photovoltaic systems, which operate optimally at flux concentrations in excess of 1000 suns. (Silicon cells would not likely benefit from dispersion compensation since they operate at much lower concentration levels.) In order to realize significant performance gains from dispersion compensation, improvements in optical tracking accuracy may also be required since tracking errors are at least as significant as chromatic dispersion in current-generation photovoltaic systems. (The effect of tracking errors would also be significant for core daylighting collectors, and methods that have been explored through Lawrence Berkeley Laboratory's core daylighting program for improving tracking accuracy might also be applicable to concentrator photovoltaics.) In addition to increasing flux concentration levels, reduced dispersion and improved tracking tolerance may also result in other benefits: The flux profile on the cell could be better controlled, and the optical performance of anti-reflection or light-trapping mechanisms or of grid line obscuration masks could be improved by reducing the focused beam's angular divergence at the cell.

For photovoltaic applications, the optical performance of a Fresnel concentrator lens can be characterized using the product of the photovoltaic cell's spectral response and the solar spectral irradiance as the spectral weighting function. Fig. 6 illustrates the wavelength dependence of ϕ_{total} for the conventional and dispersion-compensated configurations (Fig. 3) and Fig. 7 illustrates the

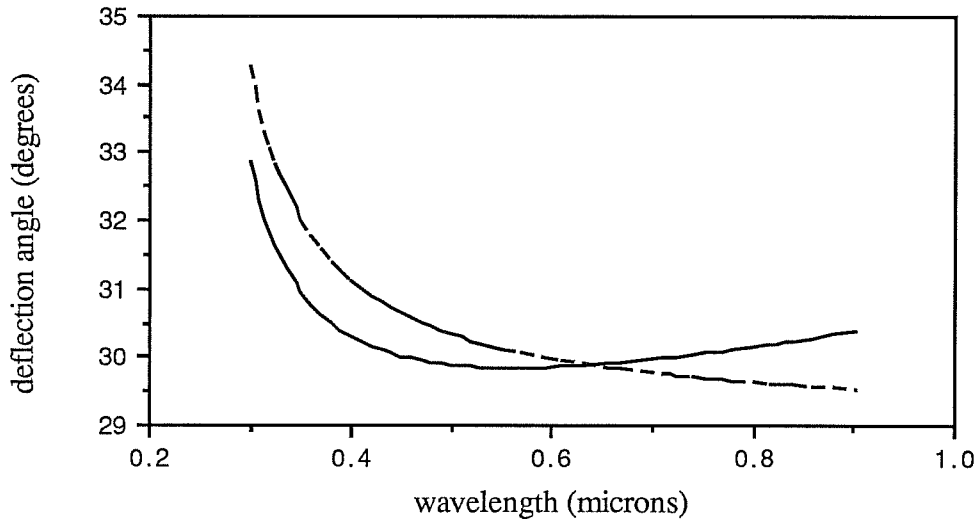


Fig. 6. Photovoltaic application: dispersion characteristic for the conventional configuration (dashed line; $\Delta\varphi_{total} = 0.492^\circ$) vs. dispersion-compensated configuration (solid line; $\Delta\varphi_{total} = 0.225^\circ$)

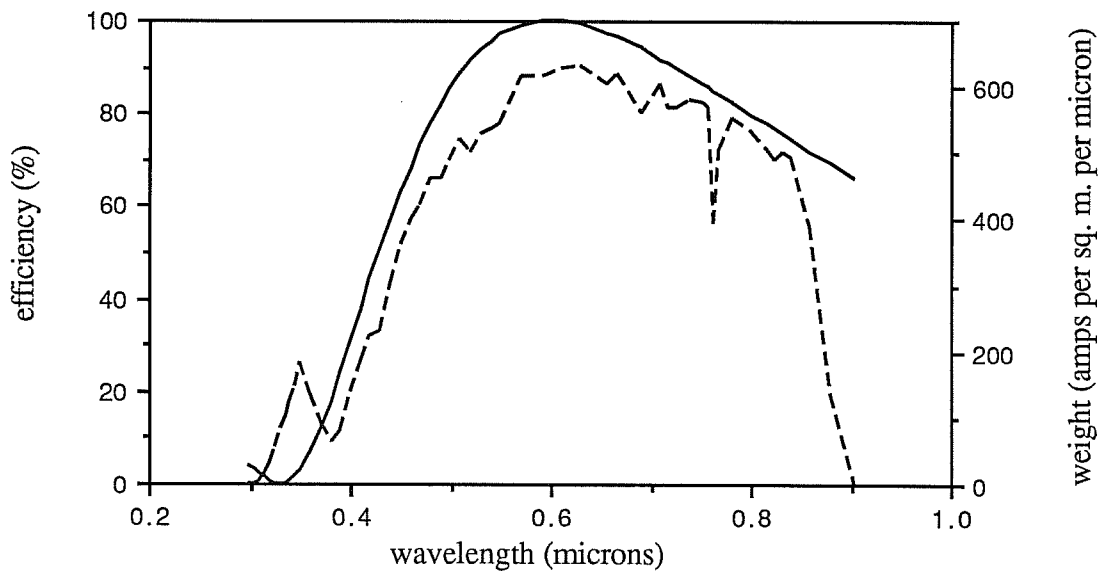


Fig. 7 Grating efficiency (solid line) vs. photovoltaic weighting function (dashed line); $\bar{\eta} = 0.843$

grating's efficiency characteristic in comparison to the weighting function for GaAs*. For the conventional configuration $\Delta\varphi_{total} = 0.492^\circ$, and with dispersion compensation $\Delta\varphi_{total} = 0.225^\circ$. The grating's diffraction efficiency is $\bar{\eta} = 0.843$; hence dispersion is reduced by a factor of 2 at a cost of 16% efficiency loss.

In practice the efficiency reduction might be less than 16% since the cell's spectral response may be increased by the grating's spectral filtering effect, which would tend to reduce heat gain in the cell. Efficiency may also be increased by other factors (e.g. the lower resistance loss of a smaller cell). The efficiency loss represents the factor by which the collector aperture area per unit power output must be increased to offset reduced optical efficiency. This loss must be balanced against the gain in flux concentration and consequent reduction in cell area per unit power output. Considering the high cost of concentrator solar cells, the cost advantage of a significant reduction in cell area might more than offset a marginal increase in collector aperture area.

3.3 Solar thermal

For solar thermal applications, a concentrator's optical performance can be characterized using the solar spectral irradiance as a weighting factor (assuming that the receiver is a blackbody absorber). Fig's. 8 and 9 illustrate a dispersion-compensating grating's comparative optical performance using this weighting function**. For the conventional configuration $\Delta\varphi_{total} = 0.616^\circ$, and with dispersion compensation $\Delta\varphi_{total} = 0.442^\circ$. The grating's efficiency is $\bar{\eta} = 0.646$. This is the diffraction efficiency in the first order - the 35% efficiency reduction represents the energy fraction diffracted into other orders, most of which would be concentrated in a diffuse halo around the first-order focused sun image. This energy would be available for capture (although its concentration level would be significantly lower than the first order's); hence the grating's practical efficiency loss may be less than 35%.

The above performance data are based on a blackbody receiver. Better efficiency and dispersion compensating performance could be obtained if the receiver's absorption spectrum is reasonably well matched to the grating's efficiency characteristic; hence the above data only represent the worst-case performance.

* For both configurations the incidence angle at the top surface is 41.21° . The prism facet angle is 52.41° for the conventional configuration and 49.79° for the dispersion-compensated configuration. The grating's period is $22.95\mu\text{m}$ and its facet angle is 2.46° . A tabulation of the data used for the spectral response of GaAs is provided in the Appendix.

** For both configurations the incidence angle at the top surface is 41.30° . The prism facet angle is 52.59° for the conventional configuration and 51.50° for the dispersion-compensated configuration. The grating's period is $78.99\mu\text{m}$ and its facet angle is 0.77° .

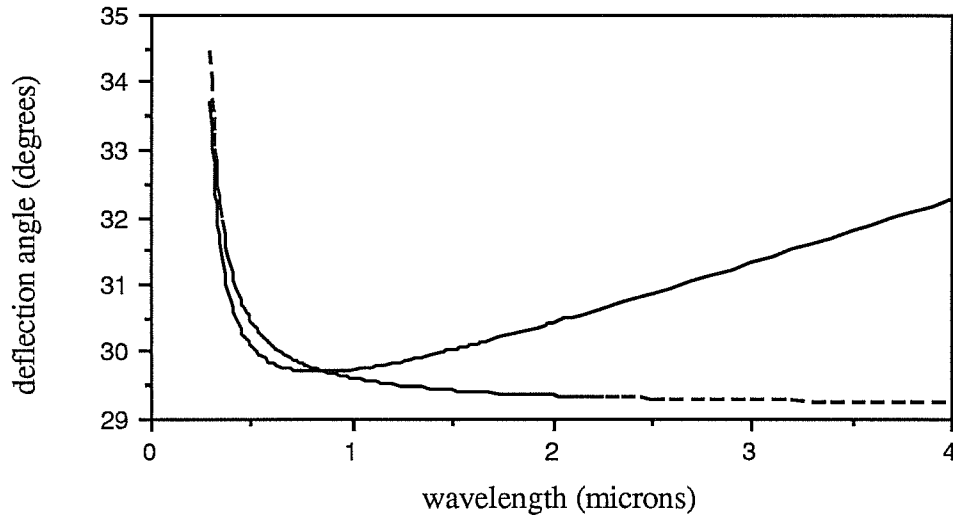


Fig. 8. Solar thermal application: dispersion characteristic for the conventional configuration (dashed line; $\Delta\varphi_{total} = 0.616^\circ$) vs. dispersion-compensated configuration (solid line; $\Delta\varphi_{total} = 0.442^\circ$)

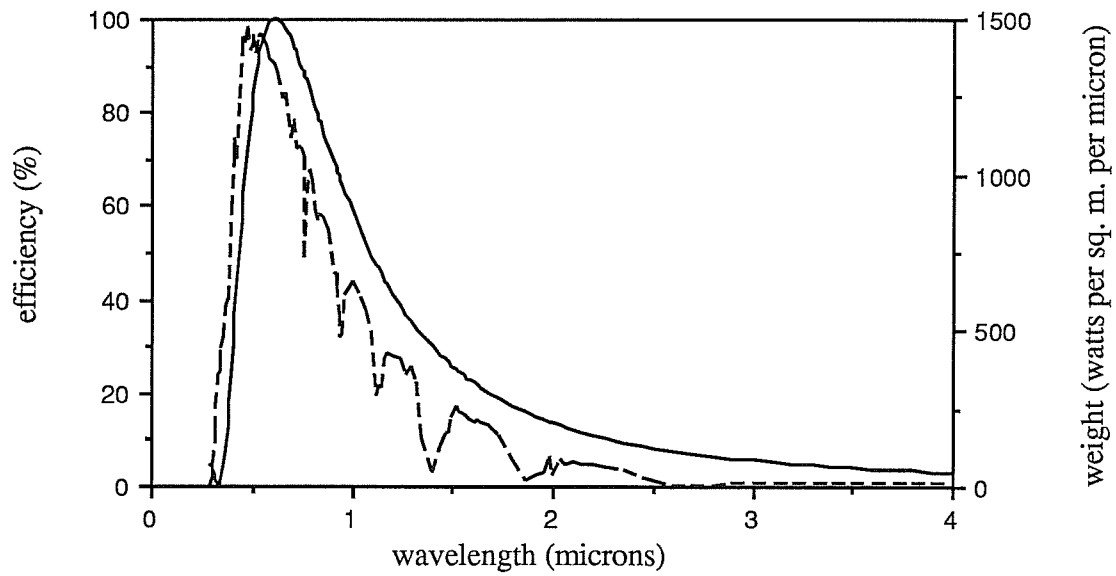


Fig. 9. Grating efficiency (solid line) vs. solar thermal weighting function (dashed line); $\bar{\eta} = 0.646$

4. REFERENCES

1. T. Stone and N. George, "Hybrid diffractive-refractive lenses and achromats," Applied Optics, vol. 27(14), pp. 2960-2971, 5 July 1988.
2. S. Mallery, "Catching some rays: New device delivers filtered sunlight indoors," Architectural Lighting, Oct. 1987, pp. 27-30.
3. S. P. Schubert, "Down the tubes: Solar light goes indoors," Architectural Lighting, Feb. 1987, pp. 32-35.
4. R. E. Bird and C. Riordan, "Simple Solar Spectral Model for Direct and Diffuse Irradiance on Horizontal and Tilted Planes at the Earth's Surface for Cloudless Atmospheres," Journal of Climate and Applied Meteorology, vol. 25(1), pp. 87-97, Jan. 1986.
5. ANSI Standard ANSI/IES RP-16-1980.
6. Technical brochure PL-165i, p. 9, published by Rohm and Haas, Philadelphia, PA 19105.

5. APPENDIX

Spectral Response of Varian GaAs concentrator cell (0.126 cm²):

λ (μ m)	Spec. Resp. (amps/watt)	λ (μ m)	Spec. Resp. (amps/watt)
0.35	0.0415	0.690	0.503
0.375	0.0949	0.710	0.515
0.40	0.157	0.730	0.527
0.425	0.211	0.750	0.535
0.450	0.262	0.770	0.539
0.470	0.297	0.790	0.552
0.490	0.330	0.800	0.543
0.510	0.359	0.812	0.567
0.550	0.376	0.828	0.575
0.570	0.436	0.844	0.565
0.590	0.449	0.860	0.450
0.610	0.463	0.876	0.204
0.630	0.476	0.892	0.0527
0.650	0.485	0.900	0.000
0.670	0.494	1.000	0.000

(source: Charles Stillwell, Sandia National Laboratory, Division 6221, Albuquerque, NM 87185.)

6. ACKNOWLEDGMENTS

This work was supported by the Assistant Secretary for Conservation and Renewable Energy, Office of Solar Heat Technologies, Solar Buildings Division of the U.S. Department of Energy under Contract No. DE-AC03-76SF00098.

I thank Steve Selkowitz for encouraging this work, and Carl Lampert for his assistance with the presentation.